# EXPERIMENTAL INVESTIGATION OF FLAT PLATE DEFLECTION UNDER VARIABLE VELOCITY PARALLEL FLOW

**J.C. Kennedy, C.J. Jesse, G.H. Schnieders, G.L. Solbrekken**
Department of Mechanical & Aerospace Engineering, University of Missouri
Lafferre Hall, Columbia, MO 65211, USA
jckx84@mail.missouri.edu; cj8q5@mail.missouri.edu; ghshy8@mail.missouri.edu;
solbrekkeng@missouri.edu

## ABSTRACT

Recent experiments using a flat, thin aluminum plate in parallel flow show a strong correlation between flow rate and plate deflection. Additionally, the plate deflection may be highly sensitive to variations in the fluid channel geometry. The geometry of interest consists of a 1.016 mm (40 mil) thick plate with channels of ideally 2.032 mm (80 mils) and 2.540 mm (100 mils) on either side. The channel/plate width was 110.287 mm (4.342 inches). A 7 kg/s Hydro-Mechanical Flow Loop at the University of Missouri acted as the test stand for these experiments.

High velocity flow through the channels caused a significant pressure differential between the channels, leading to plate deflection. A series of pressure transducers monitored the channel pressure differential, while a pair of laser displacement sensors tracked the plate deflection. Repeated experiments allowed for testing with multiple flow rates and laser measurement positions.

The free edge flow tests show measureable plate deflections occurring at total flow rates as low as approximately 1.8 kg/s. At total flow rates between 2.64 and 3.47 kg/s, the plate suddenly snapped from a static deflection in one direction to a static deflection in the opposite deflection. The snap event was clearly visible in the laser and pressure data from all experiments, and affected the entire plate at the same time. After snapping, the plate continued deflecting in the new direction as the flow rate increased.

The pinned edge flow tests saw significantly smaller deflections than the free edge tests, as would be expected. In the pinned edge tests, the largest deflections occurred away from the pinned edges. The magnitude of the deflections shows a consistent correlation with flow rate. Channel pressure differentials recorded during each flow test were largely repeatable.

By using the laser displacement sensors, mappings of the fluid channel thicknesses are available from before the experiments. These mappings show significant variation of approximately ±0.4 mm (~15 mils) in both channels. These variations may be largely responsible for the unexpected plate behavior.

**KEYWORDS**

Fluid Structure Interaction, Experiment, Flow Loop, Lasers

## 1. INTRODUCTION

As part of the Global Threat Reduction Initiative (GTRI) Reduced Enrichment for Research and Test Reactors (RERTR) program, there is an effort underway to design, test, and validate a new LEU foil based fuel for the University of Missouri Research Reactor (MURR). As part of ongoing development efforts for numeric Fluid-Structure Interaction (FSI) simulation of fuel-coolant systems, there is a need for quality, robust experimental benchmarking data. In order to generate this data, it has been necessary to develop novel techniques for characterization of the experiment geometry.

Earlier comparisons between experiments and numeric models showed a need for more detailed characterization of the experiment geometry [1] [2]. The test section is constructed with two plexi-glass panels on the outside. This allows laser displacement sensors to monitor plate deflection during a flow test. However, similar experiments conducted in 1959 showed a potential for plexi-glass to absorb water when exposed for even short periods [3]. This leads to warping of the plexi-glass, and therefore significant variability in the surface of the channels. After completing numerous flow experiments, this warping became clearly visible during test section assembly and disassembly.

In order to evaluate how the warping of the plexi-glass (and the resulting inconformity of the fluid channel thicknesses) might affect the plate deflection profile, a method was developed for mapping the fluid channels with the laser displacement sensors. This mapping process involved moving the lasers to 120 different locations in each channel and measuring the channel thickness. The resulting channel profile maps will be used in later numeric models to ensure close geometric matching between the numeric and experiment models.

In addition to mapping the channels, the lasers were used to measure the change in fluid channel thickness (i.e. plate deflection) in each channel at a single axial location during flow testing. The flow tests were repeated seven times with the lasers in a different location for each repetition. Additionally, the pressure difference between the two channels was monitored at eight axial locations during every flow test. Finally, flow rate was controlled with a bypass valve that directed flow back to the reservoir.

## 2. BACKGROUND

### 2.1. Miller Critical Velocity

Fluid-structure interaction of reactor fuel plates and coolant has been an area of study for more than half a century. In 1958, Miller proposed a method for determining a ‘Critical Flow Velocity’ based on purely analytic methods using simple beam equations and Bernoulli flow theory. Miller’s equations for critical flow velocity are shown as Eqns. 1 and 2 [4].

$$V_C = \left[\frac{15Ea^3h}{\rho b^4(1-\nu^2)}\right]^{\frac{1}{2}} \quad (1)$$

$$V_C = \left[\frac{30Ea^3h}{\rho b^4(1-\nu^2)}\right]^{\frac{1}{2}} \quad (2)$$

Where: E = Young's Modulus of Elasticity for the plate
a = Plate thickness
h = Fluid sub-channel thickness
ρ = Fluid mass density
b = Plate/fluid channel width
ν = Poisson's ratio of the plate

Equation 1 is used in the case of two or more plates, while Eqn. 2 is used if only a single plate is present. Additionally, Miller assumed a single channel thickness, h, for all channels. This differs from the experiments presented here, where the channels are intentionally made different thicknesses.

### 2.2. Earlier Experiments

In an effort to validate Miller's model, Zabriskie completed experiments in on single and multi-plate assemblies both with and without a comb. While Zabriskie did utilize plexi-glass outer panels in his experiments, they were used only for visual observation of fluid channel collapse. Additionally, through pressure measurements, Zabriskie noted in some experiments that the plate began deflecting in one direction before suddenly changing directions [5]. More recently, experiments by Liu et al. used a laser fixed at the center point of a plate to monitor plate deflection. These experiments used a semi-fixed laser and monitored the distance from the laser to the plate. These experiments were limited with the lasers fixed at a single measurement location and no pressure measurements were collected [6] [7].

## 3. EXPERIMENT APPARATUS

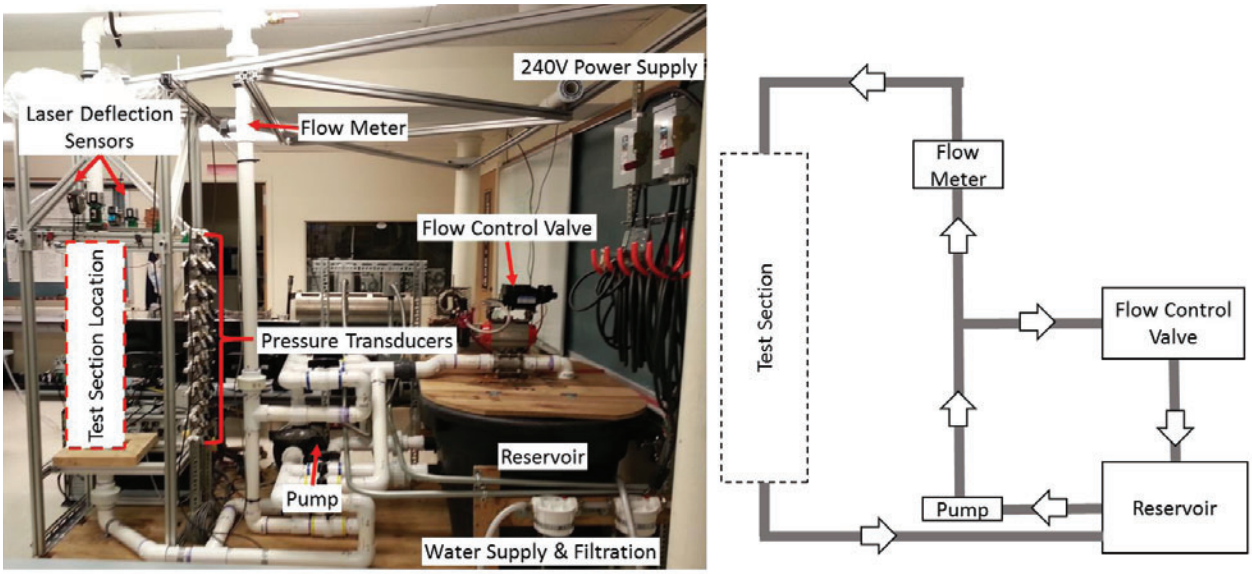


**Figure 1. University of Missouri Hydro-Mechanical Flow Loop (HMFL)**

### 3.1. Flow Loop

The Hydro-Mechanical Flow Loop (HMFL) at the University of Missouri was used for completing these experiments. The flow loop includes a National Instruments cDAQ system for data collection and flow control. User control and monitoring is accomplished with a LabView program. The flow loop and a flow path schematic is shown in Figure 1.

### 3.2. Test Section

The flow loop is designed to accommodate a wide range of test sections. The test section used for these experiments is based on a layered sandwich structure, with two outer plexi-glass panels and interior channel spacers around an Al 6061-T6 plate. A vertical cross-section showing pressure tap locations ($PT_1$ – $PT_9$) and laser measurement locations is shown in Figure 2. A horizontal cross-section demonstrating the sandwich structure of the test section is shown in Figure 3.

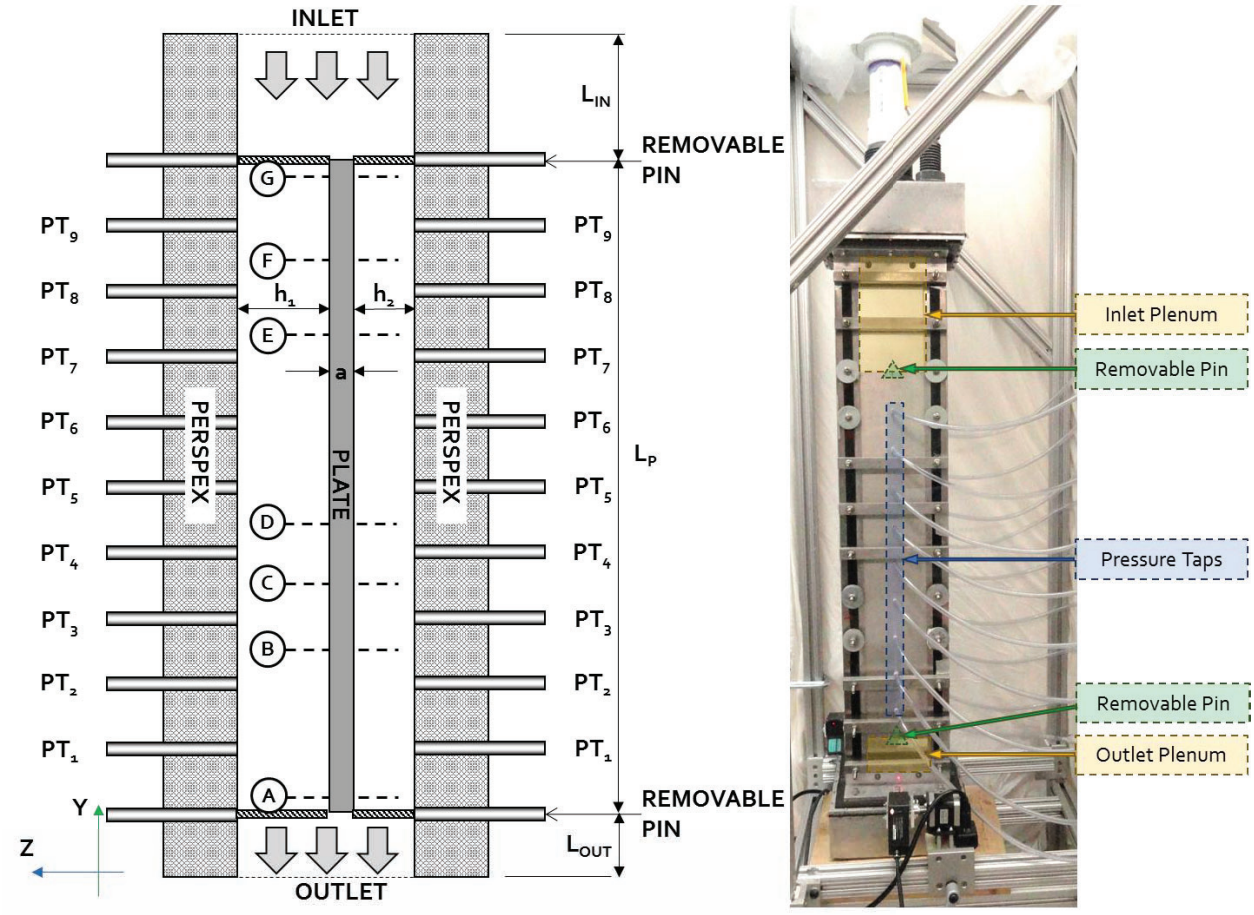


**Figure 2. Test section vertical cross-section (not to scale) and front view.**

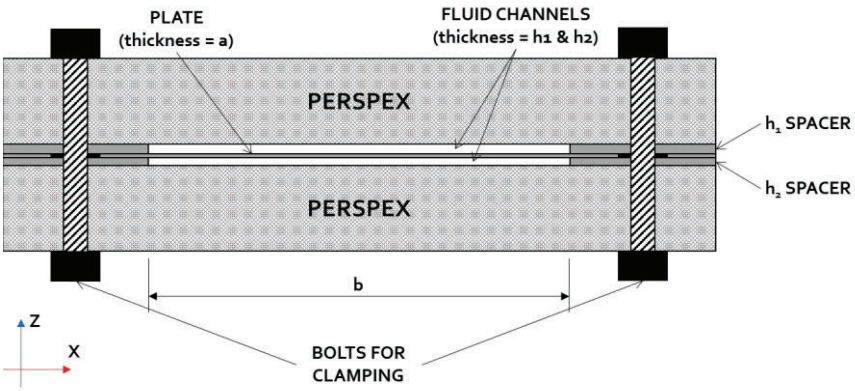


| Parameter | Design Value | |
|---|---|---|
| b | 110.287 mm | 4.342 inches |
| a | 1.016 mm | 0.040 inches |
| $h_1$ | 2.540 mm | 0.100 inches |
| $h_2$ | 2.032 mm | 0.080 inches |
| $L_{IN}$ | 190.5 mm | 7.5 inches |
| $L_P$ | 647.7 mm | 25.5 inches |
| $L_{OUT}$ | 76.2 mm | 3 inches |

**Figure 3. Test section horizontal cross-section (to scale)**

**Table I. Laser channel gap measurement location relative to plate trailing edge**

| Location ID | Axial Location (From Plate Trailing Edge) | |
|---|---|---|
| **A** | 12.7 mm | (0.500 inches) |
| **B** | 152.4 mm | (6.000 inches) |
| **C** | 226.7 mm | (8.925 inches) |
| **D** | 290.5 mm | (11.438 inches) |
| **E** | 474.3 mm | (18.675 inches) |
| **F** | 550.5 mm | (21.675 inches) |
| **G** | 635.0 mm | (25.000 inches) |

**Table II. Pressure measurement location relative to plate trailing edge**

| Pressure Tap | Distance From Trailing Edge of Plate | |
|---|---|---|
| **$PT_1$** | 64.8 mm | (2.55 inches) |
| **$PT_2$** | 129.5 mm | (5.10 inches) |
| **$PT_3$** | 194.3 mm | (7.65 inches) |
| **$PT_4$** | 259.1 mm | (10.20 inches) |
| **$PT_5$** | 323.9 mm | (12.75 inches) |
| **$PT_6$** | 388.6 mm | (15.30 inches) |
| **$PT_7$** | 453.39 mm | (17.85 inches) |
| **$PT_8$** | 518.2 mm | (20.4 inches) |
| **$PT_9$** | 582.9 mm | (22.95 inches) |

### 3.3. Laser Channel Gap Measurement

To map the thickness of the fluid channels and monitor plate deflection during a flow test, two Keyence LK-G152 laser displacement sensors were used. The sensors work by emitting a laser beam through the plexi-glass panel and monitoring the location of the reflected signal. For mapping the fluid channels, water is drained from the test section and the channels are filled with air. Reflected signals are detected at

the outer surface of the plexi-glass, inner surface of the plexi-glass, and the surface of the plate. The channel thickness is taken as the distance between the inner surface of the plexi-glass and the plate surface. Any refractive effects resulting from the emitted laser passing through the plexi-glass are canceled when the return signal passes back through the plexi-glass.

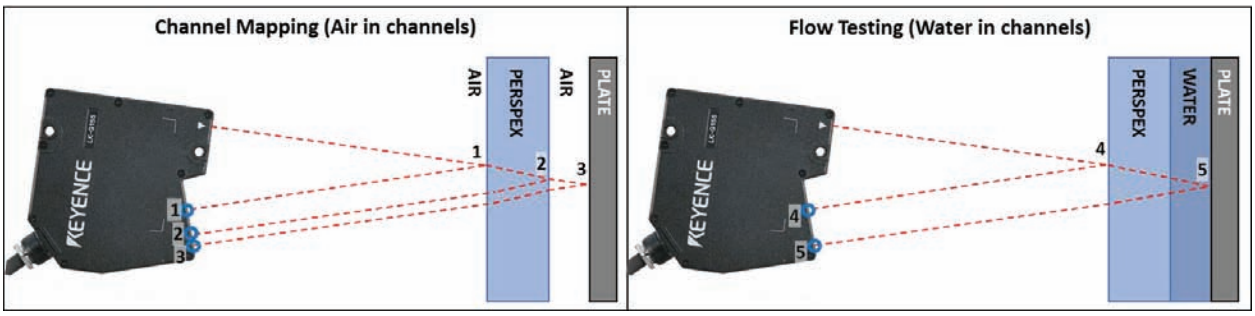


**Figure 4. Laser channel thickness measurement during mapping (left) & during flow testing (right)**

During flow testing, the fluid channels are filled with water. Since the refractive index of water and plexi-glass are so close, the lasers are unable to detect a signal from the inner surface of the plexi-glass. This results in the measurement scenario shown in right side of Figure 4. The measured signal during flow testing is the distance from the outer surface of the plexi-glass to the surface of the plate. To convert this measured signal to a usable measurement, it is therefore necessary to subtract the laser measurement of the plexi-glass thickness (points 1-2 in Figure 4), and multiply by a correction factor. The correction factor is determined by dividing the real channel gap thickness with air (points 2-3 in Figure 4) by the measured channel gap thickness with water. This results in the laser calibrations equations 3 and 4.

$$C_L = \frac{h_{2-3}}{h_{4-5} - h_{1-2}} \quad (3)$$

$$h_R = (h_{4-5} - h_{1-2}) * C_L \quad (4)$$

Where:

$C_L$= Laser correction factor
$h_{2\text{-}3}$ = Real gap thickness with air
$h_{4\text{-}5}$ = Measured plexi-glass + gap thickness with water
$h_{1\text{-}2}$ = Measured thickness of Perspex
$h_R$ = Real gap thickness with water

During flow testing, the lasers were positioned at one of the seven locations (A-G) indicated in Figure 2. Measurements of the channel gap were continuously collected at a set flow rate. After running through all 11 flow rates, the lasers were repositioned and the process was repeated at the new location.

The fluid channel gaps in the test section, while targeted to be 2.032 mm (80 mils) and 2.540 mm (100 mils), will vary from those values primarily because of assembly tolerances and past water absorption by the plexi-glass. Therefore, in order to better characterize the geometry of the channels, the laser

displacement sensors were utilized to map the thickness of the fluid channels along the grid shown in Figure 5. The channel mapping was completed prior to conducting the flow experiments.

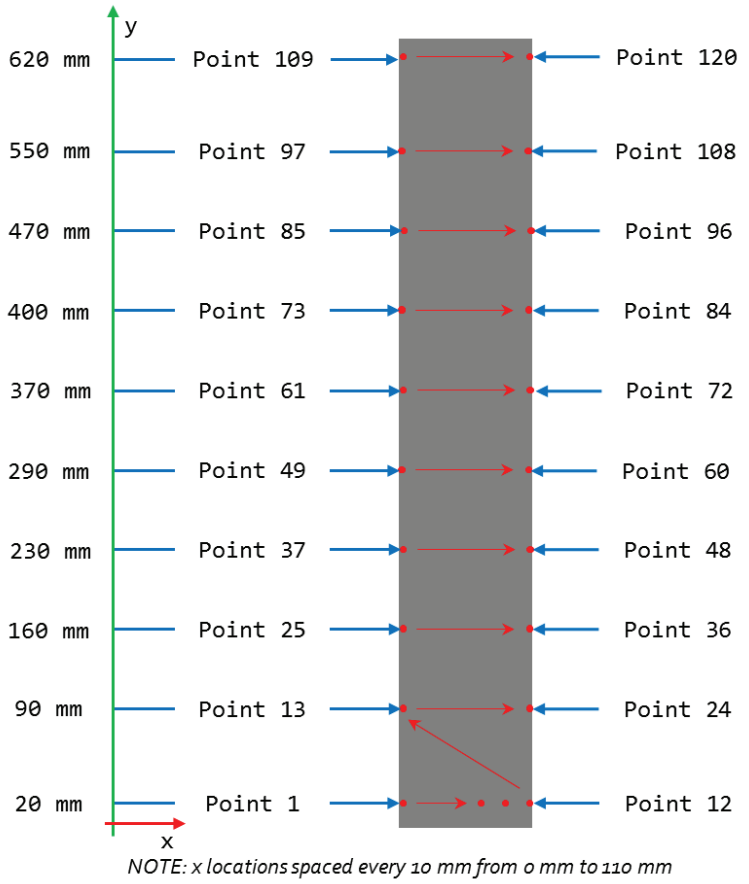


**Figure 5. Channel mapping grid**

The mapping consisted of taking measurements at 120 locations in each channel. The measurement grid consisted of 12 locations across the width (x-direction) of the plate, and 10 locations along the length (y-direction) of the plate. Each measurement consisted of 30 samples from each laser, and the process was repeated for a total of nine trials with each trial going from point 1 through point 120. The lasers were positioned horizontally with stepper motors and a LabView control program connected to an Arduino. Vertical positioning was accomplished by moving the laser assembly manually and clamping to the surrounding support structure.

### 3.4. Differential Pressure Measurement

In order to monitor the pressure difference between the two fluid channels during flow testing, the test section is equipped with nine Omega PX-26 differential pressure transducers ($PT_1$ – $PT_9$), as shown in Figure 2. The pressure transducers have been calibrated across a range of -30 kPa to +30 kPa. The pressure measurement locations are spaced at 64.77 mm (2.55 inch) increments. There are no pressure measurements at the leading and trailing edges due to the presence of screws for pinning the plate at those locations. Pressure measurements were always collected in the same locations. Since the lasers had to be

moved through seven locations, the pressure measurements were essentially repeated seven times at all 11 flow rates. This data can provide a reliable measure of the repeatability of the flow tests. Additionally, while the test section was instrumented with nine pressure transducers, $PT_8$ failed early in flow testing and no data is available from that location.

### 3.5. Flow Test Procedure

Once the lasers were positioned at the desired location, calibration measurements were taken as outlined in Eqns. 3 and 4. Then, the water was turned on and flow testing began at the lowest flow rate. After collecting data for approximately 30 seconds, the flow rate was increased by slightly closing the flow bypass valve in Figure 1. The process was repeated until data was collected at all 11 flow rates. Upon completion of the final flow rate, the water was shut off, the test section was drained, and the lasers were moved to the next measurement location where the flow test was repeated. This process was completed first with the leading and trailing edges free, and then a second time with pins at the leading and trailing edges to simulate a comb.

## 4. RESULTS

### 4.1. Channel Mapping

By repeating the mapping process nine times, it is possible to begin to understand the errors associated with the placement of the laser sensors. To understand the variation within each mapping, Figure 6 shows the mean values at each measurement location with error bars representing the minimum and maximum values. The x-axis corresponds to the measurement locations shown in Figure 5, and therefore each set of 12 points corresponds to one horizontal row on the test section. The average channel thicknesses and areas are provided in Table III.

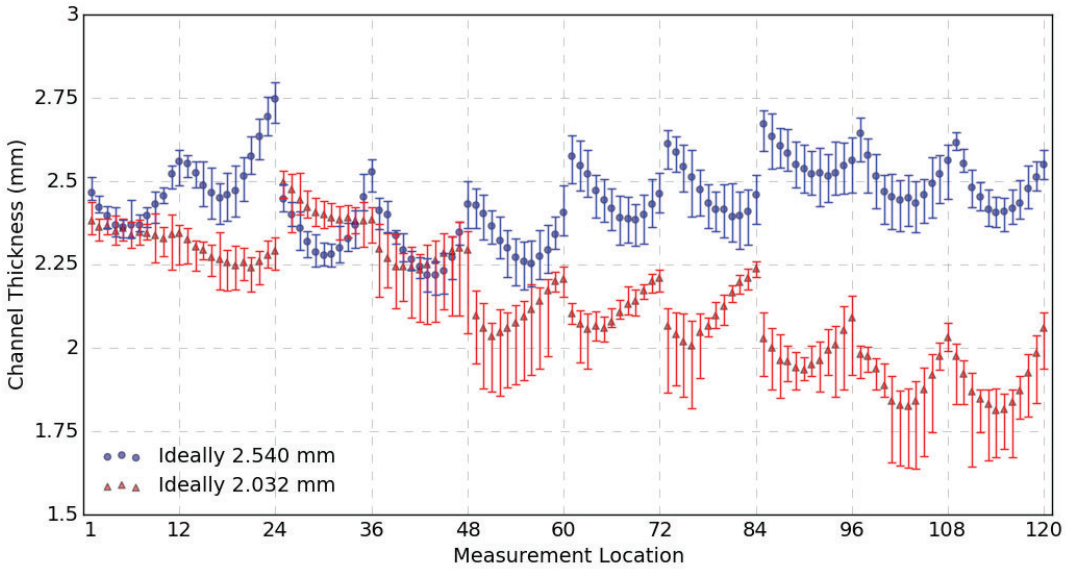


**Figure 6. Channel gap mapping mean, minimum, and maximum values**

**Table III. Ideal and measured channel thickness and area**

| Channel | Channel Thickness | | | | Channel Area | | | |
|---|---|---|---|---|---|---|---|---|
| | Ideal | | Measured | | Ideal | | Measured | |
| | mm | inch | mm | inch | $mm^2$ | $in^2$ | $mm^2$ | $in^2$ |
| **1** | 2.540 | 0.100 | 2.444 | 0.0962 | 280.128 | 0.4342 | 269.52 | 0.4178 |
| **2** | 2.032 | 0.080 | 2.143 | 0.0844 | 224.103 | 0.3474 | 236.35 | 0.3664 |
| **Total** | **4.572** | **0.180** | **4.587** | **0.1806** | **504.231** | **0.782** | **505.88** | **0.7841** |

The average of the nine measurements taken at a given location was calculated and used to generate surface plots of the channel thicknesses, shown in the left half of Figure 7. In addition to the channel thicknesses, it is helpful to know the differential in the channel thicknesses and the sum of the thicknesses. The right half of Figure 7 shows these values. Note that in the channel difference plot, the ideally larger channel is actually smaller in an area approximately 225 mm from the trailing edge of the plate. Additionally, from the channel summation plot it is clear that the channels tend to become thinner near the axial centerline of the channels. This observation has been confirmed visually during assembly of the test section, with the bowing of the panels being easily visible.

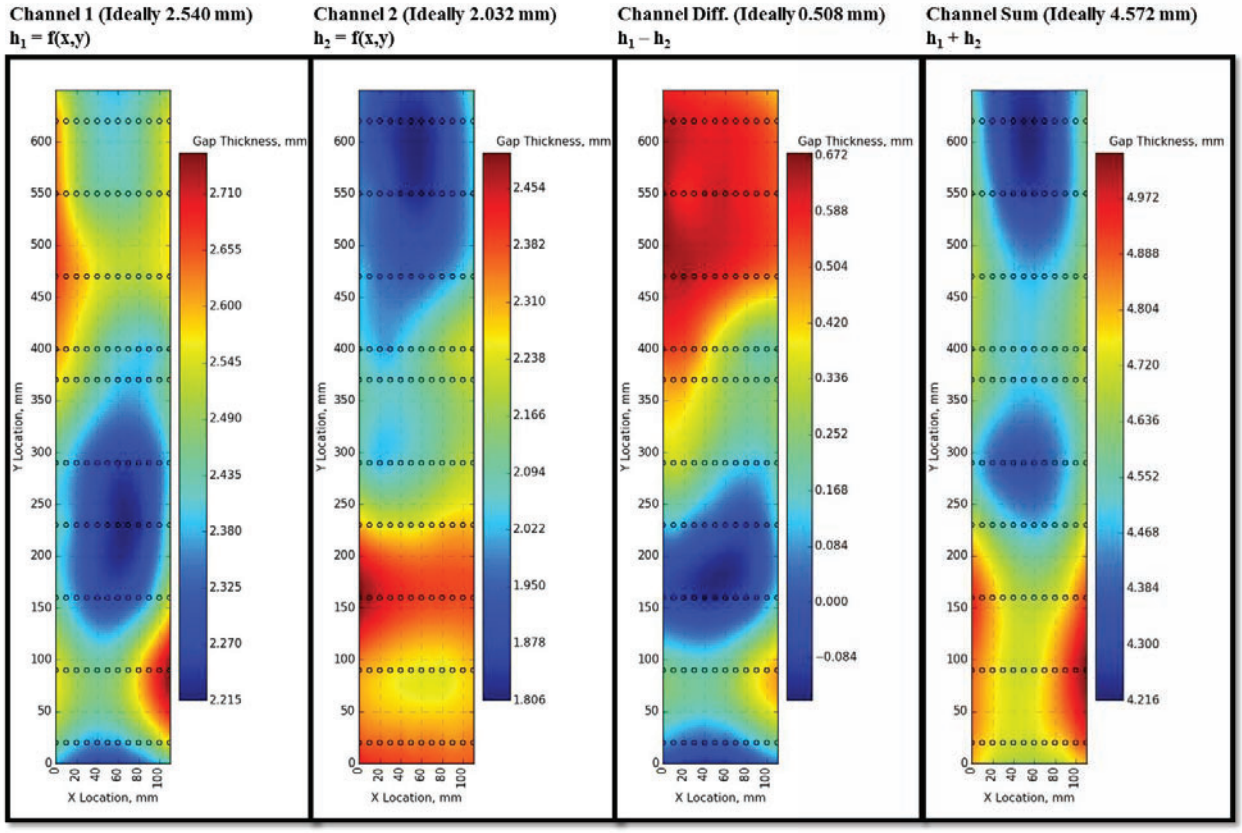


**Figure 7. Channel thickness mapping and interpolation**

### 4.2. Free Edge Flow Testing

Since the change in the channel gap thickness should correspond with the plate deflection, the initial channel gap thickness was subtracted from the gap thickness observed during flow testing. The plot in Figure 8 shows the resulting plate deflection at all seven measurement locations.

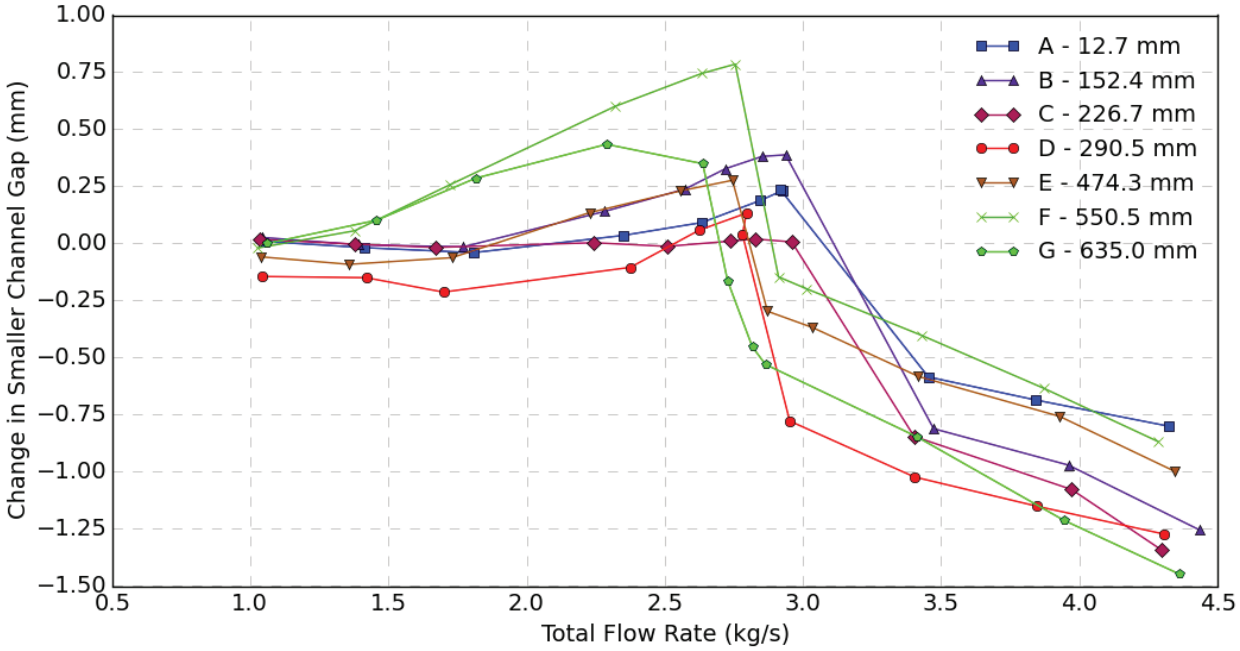


**Figure 8. Change in smaller channel gap (i.e. plate deflection) at all 7 axial measurement locations with free leading and trailing edges. Axial locations A-G are identified in Figure 2.**

During the free edge flow tests, the plate began deflecting into the larger channel, as expected. However, at flow rates between 2.64 and 3.47 kg/s, the plate would suddenly 'snap' over to the other channel. Deflection would continue in this direction as the flow rate increased. This snap was observed visually, with the lasers, and in the pressure data of Figure 9. From the pressure data, it is clear that the snap occurred at a slightly different flow rate for each trial. Despite the hysteresis in the snap velocity, the pressure data showed repeatable behavior through all seven experiment repetitions.

The pressure drop data shown in Figure 9 is the measurement of the static pressure difference between the smaller channel and the larger channel ($\Delta P = P_{small} - P_{large}$). It can be seen in the plots that the profile of the pressure difference relative to flow rate is not consistent for all axial locations at low flow rates. In some of the locations, the pressure difference decreases with increasing flow rate while other locations show the opposite trend. Then at a flow rate around 2.75 kg/s, it can be seen that there is a drastic reversal in the pressure difference. That pressure difference reversal coincides with the plate deflection data in Figure 8 that shows the snapping of the plate. At subsequently higher flow rates all pressure differences show a similar trend.

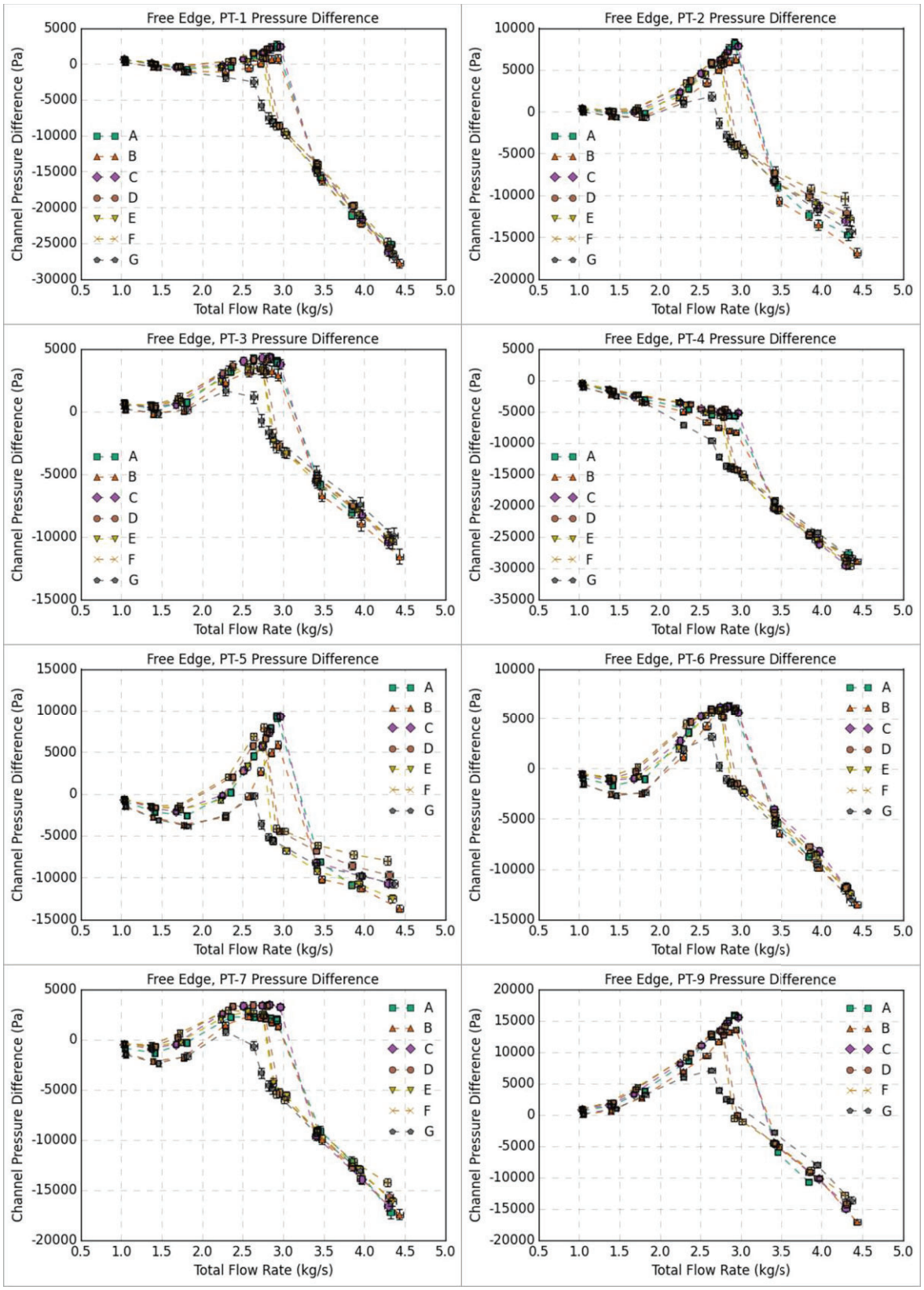


**Figure 9. Free edge experiment pressure results**

### 4.3. Pinned Edge Flow Tests

As with the free edge results, the change in the smaller channel gap at all seven measurement locations and all flow rates is shown in Figure 10. It can be seen that the magnitude of the plate deflections is markedly reduced relative to the unpinned configuration. It is also interesting to note that the plate bends into both channels as evidenced by both positive and negative channel gap changes existing at higher flow rates.

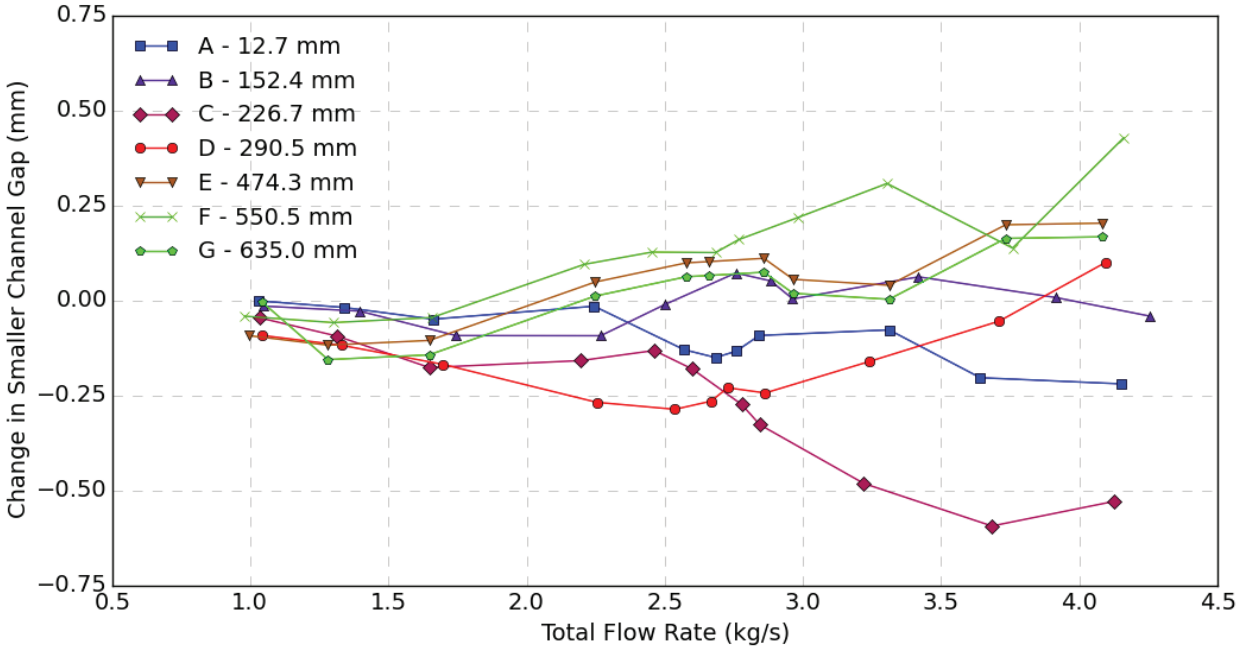


**Figure 10. Change in smaller channel gap (i.e. plate deflection) at all 7 axial measurement locations with pinned leading and trailing edges. Axial locations A-G are identified in Figure 2.**

As expected, deflections are significantly smaller with a pinned point at the center of the leading and trailing edges. However, it is interesting to note that at point G, which is only about 12 mm from the leading edge, significant deflections were observed. Given the small contact area of the pin, this deflection likely results from a slight rotation of the plate about the pinned location.

The pressure difference along the channel over the range of flow rates is shown in Figure 11. In this set of data it is apparent that there is not a dramatic snapping event like there was in the un-pinned data. It is also seen that there is no clear trend in how the pressure difference varies with the flow rate.

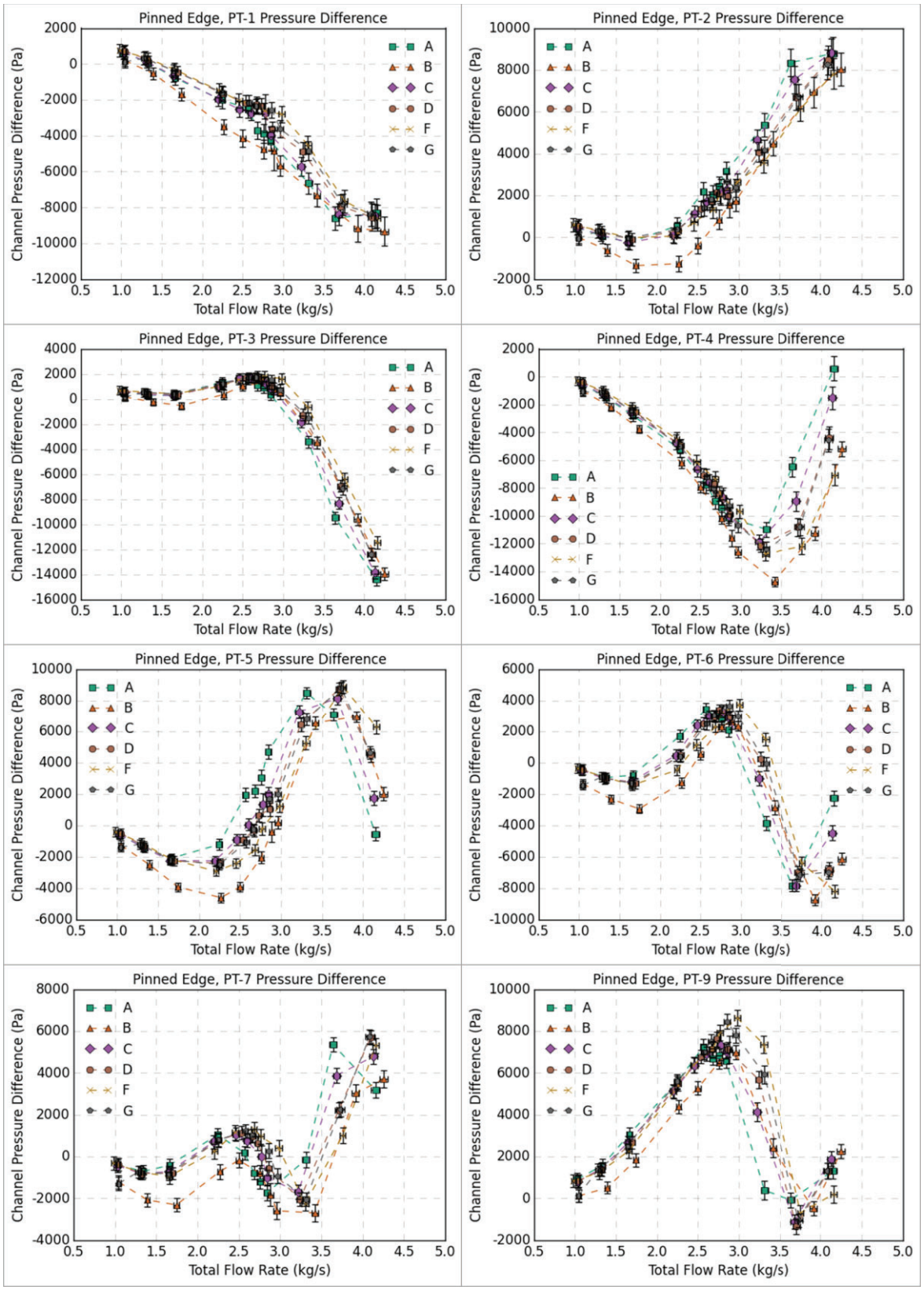


**Figure 11. Pinned edge experiment pressure results**

## 5. CONCLUSIONS

The use of the laser deflection sensors to map the fluid channels revealed much larger variances in the channel thickness than was previously expected. These variances in the channel thickness may explain the unexpected change in plate deflection direction as the flow rate increased during the free edge experiments. Additionally, integrating these measurements into future numeric models may help bring the numeric results into closer alignment with the experiment results. One remaining issue with the channel mappings is the wide variation in measured channel thickness, as seen in Figure 6. Upon investigation, it was determined these variations are likely the result of inaccuracies in positioning the lasers. As was mentioned earlier, the lasers are positioned with stepper motors in the horizontal (X) direction and manually in the vertical (Y) direction. Future mappings should consider additional automation and tighter controls when positioning the lasers.

The free edge experiments showed significant deflections, even at lower flow rates. Additionally, the sudden plate snapping from a static deflection in one direction to deflection in the opposite direction will require additional investigation. The uneven channel geometry may be responsible for the change in deflection direction at higher velocities. In order to verify this assertion, it is necessary to carry out simulations using models that match the imperfect flow channels.The pinned experiments showed much lower deflections. However, significant deflection was observed at locations near the leading edge. A larger area for the pin to contact the plate may be helpful in further minimizing deflection.

## 6. ACKNOWLEDGEMENTS

In addition to the University of Missouri, the authors would also like to thank John Stevens, Adrian Tentner, and Erik Wilson at Argonne National Laboratory for their support in this research. This work has been completed under Argonne National Lab (ANL) contract 6J-00005-0003A.

## 7. REFERENCES

[1] J. C. Kennedy, "Hydro-Mechanical Analysis of Low Enriched Uranium Fuel Plates for University of Missouri Research Reactor," University of Missouri, Columbia, MO, 2012.

[2] C. J. Jesse, J. C. Kennedy and G. L. Solbrekken, "Fluid-Structure Interaction (FSI) Modeling of Thin Plates," in *16th International Topical Meeting on Nuclear Reactor Thermalhydraulics*, Chicago, 2015.

[3] W. L. Zabriskie, "An Experimental Evaluation of the Effect of Length-to-Width Ratio on the Critical Flow Velocity of Single Plate Assemblies," General Electric General Engineering Laboratory, Schenectady, NY, 1959.

[4] D. R. Miller, "Critical Flow Velocities for Collapse of Reactor Parallel-Plate Fuel Assemblies," Knolls Atomic Power Laboratory, Schenectady, New York, 1958.

[5] W. L. Zabriskie, "An Experimental Evaluation of the Critical Flow Velocity Formulas for Parallel Plate Assemblies," General Electric General Engineering Laboratory, Schenectady, NY, 1958.

[6] L. Liu, D. Lu, Y. Li, P. Zhang and F. Niu, "Large-amplitude and narrow-band vibration phenomenon of a foursquare fix-supported flexible plate in a rigid narrow channel," *Nuclear Engineering and Design*, vol. 241, no. 8, pp. 2874-2880, 2011.

[7] Y. Li, D. Lu, P. Zhang and L. Liu, "Experimental investigation on fluid-structure interaction phenomenon caused by the flow through double-plate structure in a narrow-channel," *Nuclear Engineering and Design*, vol. 248, pp. 66-71, 2012.